FIB-NANOSIMS-TEM COORDINATED STUDY OF A WARK-LOVERING RIM IN A VIGARANO TYPE A CAI. M. Ito[1,2], S. Messenger[1], L.P. Keller[1], Z.U. Rahman[3] D.K. Ross[3] and K. Nakamura-Messenger[1,3]. [1]Robert M. Walker Laboratory for Space Science, ARES, NASA JSC, 2101 NASA Parkway, Houston TX 77058, USA. [2]LPI-USRA, [3] ESCG/ Jacobs Engineering (motoo.ito-1@nasa.gov).

Introduction: Wark-Lovering (WL) rims are thin multilayered mineral sequences that surround most Ca, Al-rich inclusions (CAIs). Unaltered WL rims are composed of the same primary high temperature minerals as CAIs, such as melilite, spinel, pyroxene, hibonite, perovskite, anorthite and olivine [e.g., 1]. It is still unclear whether the rim minerals represent a different generation formed by a separate event from their associated CAIs or are a byproduct of CAI formation [2]. Several models have been proposed for the origins of WL rims including condensation [1, 3], flash-heating [4, 5], reaction of a CAI with a Mg-Si-rich reservoir (nebular gas or solid) [5-7]; on the basis of mineralogy [1], abundances of trace elements [5], O [8, 9] and Mg [4, 10] isotopic studies.

Detailed mineralogical characterizations of WL rims at μm to nm scales have been obtained by TEM observations [e.g., 11-15], but so far no coordinated isotopic - mineralogical studies have been performed. Thus, we have applied an O isotopic imaging technique by NanoSIMS 50L [16] to investigate heterogeneous distributions of O isotopic ratios in minerals within a cross section of a WL rim prepared using a focused ion beam (FIB) instrument. After the isotopic measurements, we determine the detailed mineralogy and microstructure of the same WL FIB section to gain insight into its petrogenesis.

Here we present preliminary results from O isotopic and elemental maps by NanoSIMS and mineralogical analysis by FE-SEM of a FIB section of a WL rim in the Vigarano reduced CV3 chondrite.

Experimental: VigML2b is a small fragment of a coarse-grained type A CAI of about 100x150 μm from the reduced CV3 Vigarano chondrite (Fig. 1). The CAI includes a segment of a WL rim that is 40 x 60 μm. We selected two regions-of-interest (ROIs) #1 and #2 in Fig. 1 that have typical textures and mineralogical sequences of a WL rim.

We used the dual beam FIB instrument at the NASA JSC (FEI: Quanta 3D-FEG) to extract, *in-situ*, a cross section of the WL rim. The FIB section of the WL rim was prepared using a 30 keV focused Ga ion beam. Deposition of a ~3 μm thick C-strip protecting the chosen ROIs in the WL rim was followed by the ion beam milling of an ~5 μm thick section. The section was extracted from the bulk rim, and then attached to a OMNI half TEM grid with C (Pt) deposition. The section recovered from the WL rim had dimensions of about 15 μm in height and 60 μm in width. We used JEOL 6340F FE-SEM to obtain backscatterd electron (BSE) images and X-ray elemental images of the FIB section 1 at JSC prior to ion probe measurements.

O isotopic maps of the WL rim thin section were obtained using the JSC NanoSIMS 50L following techniques described in [16]. A focused Cs^+ primary ion beam with a diameter of ~100 nm was rastered over 18 x 18 μm. Secondary ion images of $^{16}O^-$, $^{18}O^-$, $^{28}Si^-$, $^{24}Mg^{16}O^-$, $^{27}Al^{16}O^-$ and $^{40}Ca^{16}O^-$ were acquired simultaneously in multidetection with EMs at a high mass resolution of ~9500. San Carlos olivine was measured as an isotopic standard. A normal incident electron gun was applied to prevent charging of the rastered area.

Results and Discussions: Figure 2a shows a BSE image of FIB-lift-out section from ROI #1 in Fig. 1. The mineralogical sequence consists of melilite (Ak5), hibonite, perovskite, spinel, fine-grained anorthite + pyroxene + spinel mixture, and Al-rich diopside layers from the interior toward to the edge (Fig. 2b). The O isotopic compositions of individual layers in the section show ^{16}O enrichments (Fig. 2c). Oxygen isotopic ratios in each mineral were calculated from Fig 2c, and matched values in previous studies [e.g., 7, 8]; spinel, hibonite, perovskite, melilite Ak5, and Ak20 had a $\delta^{18}O$ of -40, -40, -37, -22 and -17 ‰, respectively. Notably, we found a ^{16}O-poor layer between ^{16}O-rich spinel and diopside layers (Fig. 2c). The ^{16}O-poor layer is an aggregate of fine minerals, anorthite, spinel and diopside. This layer shows two different O isotopic compositions: one is an ^{16}O-poor (~ +3 ‰) Si- and Al-rich phase and the other is moderately ^{16}O-rich (~ -12 ‰) and is a Si-rich, Al-poor phase. The diopside layer at the edge of the rim has an ^{16}O-enrichment of -

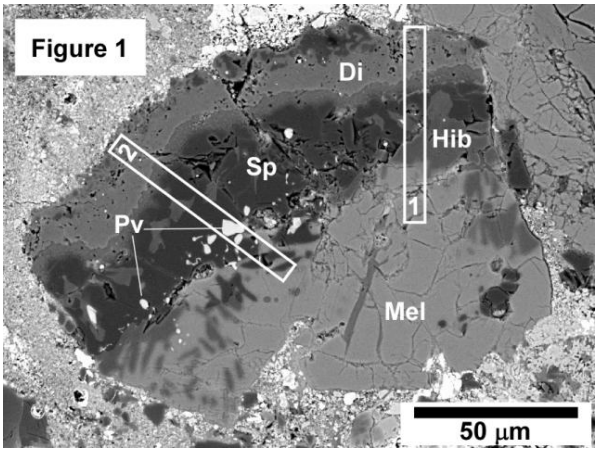

20‰ with large error. Our results support previous [e.g., 8, 9, 17] O isotopic studies of WL rims that suggested WL rims crystallized from the same ^{16}O-rich environment from which CAIs formed.

Traverse isotopic imaging of the rim shows the O isotopic compositions vary from ^{16}O-rich to ^{16}O-poor back to ^{16}O-rich. This observation suggests that the formation of the WL rim occurred as the CAI cycled between ^{16}O-rich and ^{16}O-poor regions of the nebula implying a multi-stage formation processes for the WL rim. This is consistent with a previous study which showed that Allende CAI formation began in ^{16}O-rich and subsequently continued in ^{16}O-poor region [17].

These results may be explained by flash heating and subsequent reequilibration with ambient Mg, Si rich nebular gas or melt [7]. Shock waves [18] or flares near the active proto-sun [19, 20] at a CAI-forming region models are possible settings for intermittent high temperature processes.

Further coordinated investigations of detailed microstructure, chemical compositions, and interrelationships at the µm- to nm-scale by TEM, and Mg isotopes and trace element (REEs) mapping of a WL rim by NanoSIMS are planned to improve our understanding of the formation process, time scale and origin of WL rims.

References: [1] Wark D.A. and Lovering J.F. (1977) *LPS* 8, 95-112. [2] MacPherson G.J. (2004) Treatise on Geochemistry, 201-246. [3] Ciesla F.J. et al. (2003) *Science* 299, 549-552. [4] Simon J.I. et al (2005) *Earth Planet. Sci. Lett.*, 238, 272-283. [5] Wark D. and Boynton W. (2001) *Meteoritics & Planet. Sci.*, 36, 1135-1166. [6] MacPherson G.J. et al. (1981) *LPS* 12, 648-650. [7] Ruzicka A. (1997) *JGR* 102, 13387-13402. [8] Cosarinsky M. et al (2008) *GCA* 72, 1887-1913. [9] Yoshitake et al (2005) *GCA* 60, 2663-2674. [10] Taylor D.J. et al (2005) *LPS* 36, 2121. [11] Keller L.P. and Buseck P.R. (1989) *LPS* 20, 512. [12] Keller L.P. and Buseck P.R. (1994) *Am. Mineral.* 79, 73-79. [13] Toppani A. et al. (2005) *LPS* 37, 2030. [14] Stroud R.M. et al. (2007) *Workshop on Impact Cratering II*, 4078. [15] Zega et al. (2009) *Meteoritics & Planet. Sci.*, A226. [16] Ito and Messenger (2008) *Appl. Surf. Sci.*, 255, 1446-1450. [17] Ito and Messenger (2008) *Meteoritics & Planet. Sci.*, A65. [18] Desch S.J. and Connolly H.C. (2002) *Meteoritics & Planet. Sci.*, 37, 183-207. [19] Shu F.H. et al. (2001) *Astrophys. J.*, 548, 1029-1050. [20] Itoh S. and Yurimoto H. (2003) *Nature* 423, 728-731.

Figure 2

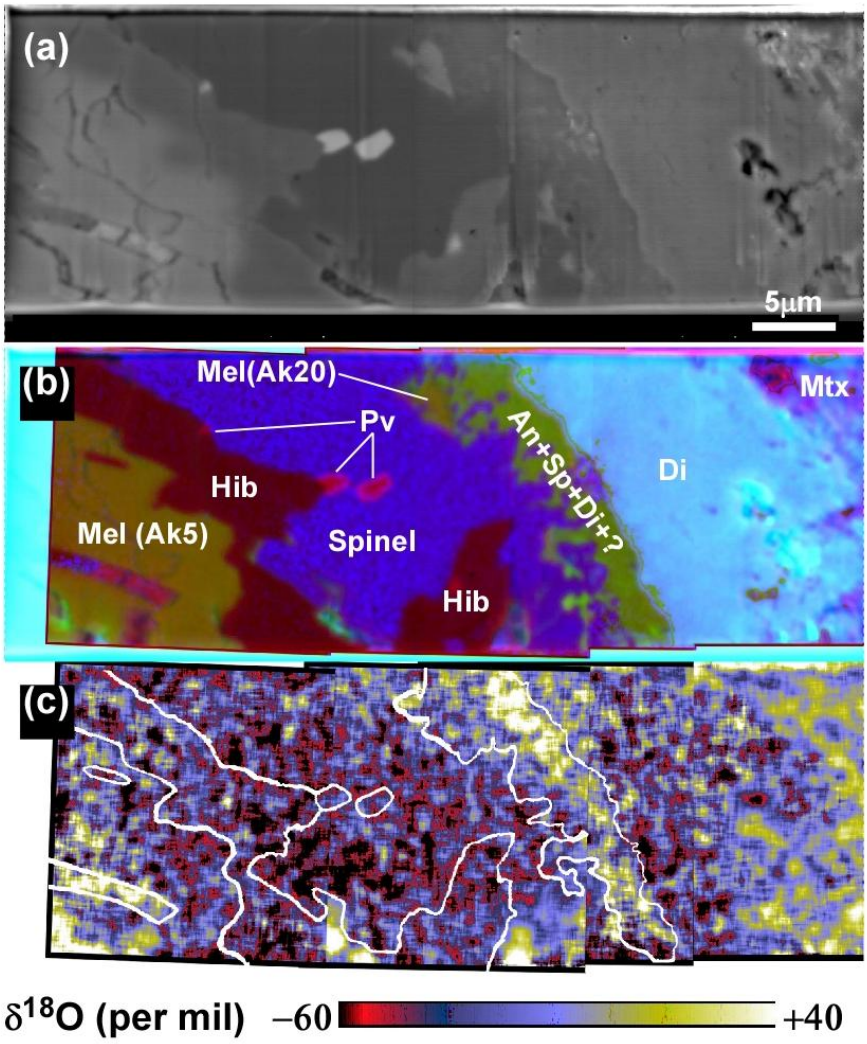

Figure 2. FIB section from ROI 1 in Fig.1. (a) BSE image of a WL rim FIB section of a Vigarano Type A CAI. (b) Mineral image generated from MgO^-/AlO^-, Si^-/O^- and BSE images. (c) $\delta^{18}O$ isotopic map (-60 to +40 ‰). White outlines indicate area of minerals. Field of view of images is 15 x 60 µm. An: anorthite; Di: Al-rich diopside; Hib: hibonite; Mel: melilite; Mtx: Matrix; Pv: perovskite; Sp: spinel.